Water Science & Technology

IWA PUBLISHING

Water Science & Technology Vol 87 No 8, 1925 doi: 10.2166/wst.2023.114

Rate constants for the reactions of chloride monoxide radical (ClO$^{\bullet}$) and organic molecules of environmental interest

László Wojnárovits and Erzsébet Takács *

Radiation Chemistry Department, Institute for Energy Security and Environmental Safety, Centre for Energy Research, H-1121, Konkoly-Thege Miklós út 29-33, Budapest, Hungary
*Corresponding author. E-mail: takacs.erzsebet@ek-cer.hu

ET, 0000-0003-3872-1615

ABSTRACT

ClO$^{\bullet}$ plays a key role in the UV/chlorine process besides Cl$^{\bullet}$, Cl2$^{\bullet}$ −, and $^{\bullet}$OH. In many experiments, ClO$^{\bullet}$ proved to be the main reactant that destroyed the organic pollutants in advanced oxidation process. About 200 rate constants of ClO$^{\bullet}$ reactions were collected from the literature, grouped together according to the chemical structure, and the molecular structure dependencies were evaluated. In most experiments, ClO$^{\bullet}$ was produced by the photolytic reaction of HClO/ClO−. For a few compounds, the rate constants were determined by the absolute method, pulse radiolysis. Most values were obtained in steady-state experiments by competitive technique or by complex kinetic calculations after measuring the pollutant degradation in the UV/chlorine process. About 30% of the listed rate constant values were derived in quantum chemical or in structure-reactivity (QSAR) calculations. The values show at least six orders of magnitude variations with the molecular structure. Molecules having electron-rich parts, e.g., phenol/phenolate, amine, or sulfite group have high rate constants in the range of 10^8–10^9 mol^{-1} dm^3 s^{-1}. ClO$^{\bullet}$ is inactive in reactions with saturated molecules, alcohols, or simple aromatic molecules.

Key words: ClO$^{\bullet}$ radical reactivity, competitive technique, pollutant degradation, structure dependence, UV/chlorine process, wastewater

HIGHLIGHTS

- ClO$^{\bullet}$ has high rate constants with molecules having electron-rich activated parts.
- ClO$^{\bullet}$ has low reactivity with saturated molecules, alcohols, and simple aromatics.
- For most compounds, only one published value is available.
- Values obtained in different laboratories show a large scatter.

INTRODUCTION

In the UV/chlorine process, several radical species contribute to the degradation of organic pollutants (De Laat & Stefan 2018); the most important ones are chlorine atom (Cl$^{\bullet}$), dichloride radical anion ($Cl_2^{\bullet-}$), chlorine monoxide radical (ClO$^{\bullet}$) (with common name reactive chlorine species (RCS)) and hydroxyl radical ($^{\bullet}$OH). We collected the reduction potential values of these radicals in Table 1, the ClO$^{\bullet}$/ClO$^-$ couple has the lowest value, 1.39 V vs. NHE (Armstrong *et al.* 2015), and consequently, it has the smallest oxidation capacity. As the source of active radicals, hypochlorite is added to the solutions. Hypochlorite also forms when chlorine (Cl_2) is dissolved in water (Reactions (1) and (2)). Cl$^{\bullet}$ together with $^{\bullet}$OH forms in the photoreaction of HClO and ClO$^-$ (Reactions (3)–(5)). In the presence of a sufficient concentration of chloride ions (Cl$^-$) in water, there is a dimerization and $Cl_2^{\bullet-}$ radical ion forms (Reaction (6)). $Cl_2^{\bullet-}$ participation in chemistry is characteristic of the low pH values (pH < 6). At high pH, $Cl_2^{\bullet-}$ transforms to $^{\bullet}$OH (Wojnárovits & Takács 2021, 2022). These oxidizing radicals (Cl$^{\bullet}$ and $^{\bullet}$OH) react with organic molecules in radical addition to the double bonds, in H-atom abstraction

Table 1 | Reduction potentials of inorganic couples vs. NHE (Armstrong *et al.* 2015)

Redox couple	Reduction potential, V
$Cl^{\bullet}/Cl^{-}$	2.43
$Cl_2^{\bullet-}/2Cl^{-}$	2.1
$ClO^{\bullet}/ClO^{-}$	1.39
$^{\bullet}OH/OH^{-}$	1.9

from the saturated parts of molecules, or by single electron transfer (SET) reaction ($Cl^{\bullet}$, $Cl_2^{\bullet-}$).

$$Cl_2 + H_2O \rightarrow HOCl + H^+ + Cl^- \quad (1)$$

$$HOCl \rightleftharpoons ClO^- + H^+ \quad (pK_a = 7.5) \quad (2)$$

$$HOCl \xrightarrow{h\nu} Cl^{\bullet} + {}^{\bullet}OH \quad (3)$$

$$ClO^- \xrightarrow{h\nu} Cl^{\bullet} + O^{\bullet-} \quad (4)$$

$$O^{\bullet-} + H_2O \rightarrow {}^{\bullet}OH + OH^- \quad (pK_a = 11.9) \quad (5)$$

$$Cl^{\bullet-} + Cl^- \rightleftharpoons Cl_2^{\bullet-} \quad (6)$$

$ClO^{\bullet}$ forms in the reaction $^{\bullet}OH$ or $O^{\bullet-}$ with hypochlorite ions/hypochlorous acid (ClO^-/HOCl) (Reactions (7) and (8)). Under practical water treatment applications $ClO^{\bullet}$ may also be produced in the reactions of several other radicals, e.g., $CO_3^{\bullet-}$ (Reaction (9), Alfassi *et al.* 1988; Huie *et al.* 1991), since its reduction potential is smaller than the reduction potentials of many other radicals participating in the chemistry during water treatment in advanced oxidation processes. The chemistry of $ClO^{\bullet}$ is less known as the chemistries of $Cl^{\bullet}$, $Cl_2^{\bullet-}$ or $^{\bullet}OH$ (Neta *et al.* 1988).

$$^{\bullet}OH + ClO^- \rightarrow OH^- + ClO^{\bullet} \quad k = 9.0 \times 10^9 \text{ mol}^{-1} \text{ dm}^3 \text{ s}^{-1} \quad (7)$$

$$^{\bullet}OH + HOCl \rightarrow H_2O + ClO^{\bullet} \quad k = 2.0 \times 10^9 \text{ mol}^{-1} \text{ dm}^3 \text{ s}^{-1} \quad (8)$$

$$CO_3^{\bullet-} + ClO^- \rightleftharpoons CO_3^{2-} + ClO^{\bullet} \quad k_9 = 5.4 \times 10^5 \text{ mol}^{-1} \text{ dm}^3 \text{ s}^{-1} \quad (9)$$

$$k_{-9} = 6 \times 10^2 \text{ mol}^{-1} \text{ dm}^3 \text{ s}^{-1} \quad (-9)$$

The chlorine monoxide radical ($ClO^{\bullet}$), similar to the mentioned other three radicals is considered to be a one-electron oxidant (Alfassi *et al.* 1988; Armstrong *et al.* 2015; Guo *et al.* 2017). Due to its lower reactivity as the other three, the concentration of $ClO^{\bullet}$ during the UV/chlorine process has been reported to be several orders of magnitude higher than those of $Cl^{\bullet}$ and $^{\bullet}OH$ (Zheng *et al.* 2020; Li *et al.* 2021a). Because of technical reasons, much fewer rate constant values are published for this radical than for the other radicals mentioned. The $ClO^{\bullet}$ radicals dimerize in a very fast reaction forming Cl_2O_2 (Reaction (10)). This reaction has been the subject of many investigations and the average of a large number of rate constant values is around 2.5×10^9 mol^{-1} dm^3 s^{-1} (Neta *et al.* 1988).

$$ClO^{\bullet} + ClO^{\bullet} \rightarrow Cl_2O_2 \quad (10)$$

TECHNIQUES FOR MEASURING THE RATE CONSTANTS OF CLO• REACTIONS

In their classic paper, Alfassi *et al.* (1988) used Reactions (7) and (8) to produce $ClO^{\bullet}$ and determined the rate constants in pulse radiolysis experiments. The radiolysis of water supplied $^{\bullet}OH$. In transient measurements carried out by pulse radiolysis or (laser) flash photolysis $ClO^{\bullet}$ exhibits weak light absorption with the maximum at 280 nm and molar absorbance of ~900 mol^{-1} dm^3 cm^{-1} (Alfassi *et al.* 1988). Due to the very weak absorbance of $ClO^{\bullet}$, in transient kinetic measurements the product absorbance is used in rate constant determination. However, there is a complication: HClO/ClO^- ($pK_a = 7.5$) is also an

oxidant, which reacts with many organic molecules. Alfassi *et al.* (1988) selected several organic molecules/ions (among others 4-cyanophenoxide ion, 4-nitrophenoxide ion, 4-methoxybenzyl alcohol) which had low reactivity with ClO^- and determined their rate constants at high pH. The reactivity of ClO^- is smaller than that of HClO. In the later rate constant determinations, the authors usually disregarded this reaction possibility, although many rate constant measurements were made at slightly alkaline pH (8.4).

Most of the experimentally determined rate constants published on $ClO^\bullet$ reactions were obtained in UV/chlorine experiments for the radical production and using competitive kinetics for calculation of the rate constants. The authors tried to establish reaction conditions, under which $ClO^\bullet$ was the main reactive intermediate reacting with the solute of interest. As we mentioned earlier, UV photolysis of $ClOH/ClO^-$ produces both $^\bullet OH$ and $Cl^\bullet$ (Reactions (3)–(5)). $Cl^\bullet$ has a rather colourful chemistry in such systems (Wojnárovits & Takács 2022). At relatively high $HOCl/ClO^-$ concentration, $Cl^\bullet$ mainly disappears in reaction with $HOCl/ClO^-$ ((11) and (12)). At low $HOCl/ClO^-$ and high Cl^- concentration the (6) dimerization reaction dominates. In addition to the reactions of $^\bullet OH$ ((7) and (8)) the $Cl^\bullet$ reactions also contribute to the formation of $ClO^\bullet$ ((11) and (12)).

$$Cl^\bullet + HOCl \rightarrow ClO^\bullet + Cl^- + H^+ \quad k = 3.0 \times 10^9\ mol^{-1}\ dm^3\ s^{-1} \tag{11}$$

$$Cl^\bullet + OCl^- \rightarrow ClO^\bullet + Cl^- \quad k = 8.2 \times 10^9\ mol^{-1}\ dm^3\ s^{-1} \tag{12}$$

A large number of rate constants were determined under steady-state conditions using Equation (13). In the competitive method, the rate constant relative to a reference compound is obtained. The absolute value is calculated by multiplying the relative value with the known rate constant of the competitor. In Equation (13), S and C stand for the target and competitor molecules, $k_{ClO^\bullet,S}$ and $k_{ClO^\bullet,C}$, respectively, are used for the rate constants. $[S]_0$ and [S], $[C]_0$ and [C] represent the concentrations at the beginning and after time t, respectively.

$$\ln\frac{[S]_0}{[S]} = \frac{k_{ClO^\bullet,S}}{k_{ClO^\bullet,C}} \ln\frac{[C]_0}{[C]} \tag{13}$$

The most often applied reference compounds are 1,4-dimethoxybenzene with $k_{ClO^\bullet} = 2.1 \times 10^9\ mol^{-1}\ dm^3\ s^{-1}$ and 2,5-dimethylbenzoate ion with $k_{ClO^\bullet} = 7.0 \times 10^8\ mol^{-1}\ dm^3\ s^{-1}$ (Alfassi *et al.* 1988). Guo *et al.* (2018) used gemfibrozil as a reference compound with $k_{ClO^\bullet} = 4.16 \times 10^8\ mol^{-1}\ dm^3\ s^{-1}$. The latter value was obtained also in competitive experiments in previous papers of the authors. They added NaClO to the solutions at a slightly alkaline pH (8.4) and prepared $ClO^\bullet$ by the UV photolysis of ClO^- (Reaction (4), followed by (5), (7) or (8)). The reaction mixture also contained HCO_3^-, which was assumed to remove $Cl^\bullet$, $Cl_2^{\bullet-}$ and $^\bullet OH$ (Reactions (14)–(16)), but was assumed to have low reactivity with $ClO^\bullet$ (Buxton *et al.* 1988; Neta *et al.* 1988; Mertens & von Sonntag 1995). The carbonate radical anion ($CO_3^{\bullet-}$), as it was mentioned before, in reaction with ClO^- also produces $ClO^\bullet$, although the rate constant is low (Reaction (9)) (Alfassi *et al.* 1988; Huie *et al.* 1991). In the experiments of Guo *et al.* (2017, 2018) the main radical species in the solution was $ClO^\bullet$. Kim *et al.* (2020), Kong *et al.* (2018a, 2018b, 2020a, 2020b) and Wu *et al.* (2017) also used the competitive method for rate constant determination.

$$Cl^\bullet + HCO_3^- \rightarrow H^+ + Cl^- + CO_3^{\bullet-} \quad k = 2.2 \times 10^8\ mol^{-1}\ dm^3\ s^{-1} \tag{14}$$

$$Cl_2^{\bullet-} + HCO_3^- \rightarrow H^+ + 2Cl^- + CO_3^{\bullet-} \quad k = 8.0 \times 10^7\ mol^{-1}\ dm^3\ s^{-1} \tag{15}$$

$$^\bullet OH + HCO_3^- \rightarrow H_2O + CO_3^{\bullet-} \quad k = 8.5 \times 10^6\ mol^{-1}\ dm^3\ s^{-1} \tag{16}$$

Li *et al.* (2021a), Peng *et al.* (2022) and An *et al.* (2022) used quantum chemical calculations (DFT, density functional theory) for the determination of rate constants for a large number of organic molecules. Guo *et al.* (2018), besides experimental rate constant determinations, also used structure-reactivity correlations, applying the Hammett substituent constants to predict $k_{ClO^\bullet}$ values. The same technique was employed by Sun *et al.* (2016) and Huang & Zhang (2022). The reduction potentials were also used for estimations of rate constants in $ClO^\bullet$ reactions.

Zhou *et al.* (2019) determined the rate constants for the reaction with substituted benzoic acids by modeling calculations with the involvement of a large number of reactions of the active chlorine species during the UV/chlorine process. This technique was also applied for rate constant determination in several other works.

Compilation of the published rate constants collected from original publications is given in the tables. The pH values and the accuracies are indicated as they were published in the original works. The error bounds in tables represent the σ-level uncertainty. All of the rate constant determinations were made around room temperature. The tables show also the pK_a values of compounds collected from several publications, e.g., Perrin (1965), Babic *et al.* (2007), and Shalaeva *et al.* (2008). The methods of $k_{ClO^\bullet}$ determinations are indicated by the following abbreviations: PR, pulse radiolysis; FP, flash photolysis; Comp., competitive method; Model./Fit./Simul., modeling/fitting/simulation in complex reaction systems often taking into account large numbers of reactions (usually UV/chlorine), Est./Pred./Assum. estimated/predicted/assumed based on the rate constant of structurally similar compounds (e.g., using the Hammett substituent constants), Calc., quantum chemical calculations.

RATE CONSTANTS OF DIFFERENT GROUPS OF MOLECULES

Small inorganic and organic molecules

$ClO^\bullet$ reacts with azide (N_3^-), chlorite (ClO_2^-) and ozonide (O_3^-) ions in (SET reactions with rate constants in the range of 10^8–10^9 mol^{-1} dm^3 s^{-1} (Table 2) (Klaening *et al.* 1984; Alfassi *et al.* 1988). We show this reaction in the example of N_3^- in Equation (17):

$$ClO^\bullet + N_3^- \rightarrow ClO^- + N_3^\bullet \quad (17)$$

The reaction is made possible by the lower standard reduction potential of the $N_3^\bullet/N_3^-$ couple (1.33 V vs. NHE, Armstrong *et al.* 2015) than that of the $ClO^\bullet/ClO^-$ couple (1.39 V). However, due to the small difference in the reduction potentials, the electron transfer rate constant is relatively small, $2.5 \pm 0.5 \times 10^8$ mol^{-1} dm^3 s^{-1}. The azide radical is considered to be a highly selective one-electron oxidant (Alfassi & Schuler 1985). The rate constant of carbonate ion with $ClO^\bullet$ is very low,

Table 2 | Small inorganic and organic molecules

Compound	$k_{ClO^\bullet}$, mol^{-1} dm^3 s^{-1}	Method, pH	Reference
Azide ion (N_3^-)	$2.5 \pm 0.5 \times 10^8$	PR, 11	Alfassi *et al.* (1988)
Chlorite ion, ClO_2^-	9.4×10^8	PR, 10	Alfassi *et al.* (1988)
Chlorine dioxide, ClO_2	7.4×10^9	Est.	Quiroga & Perissinotti (2005)
Ozonide ion	1.0×10^9	FP	Klaening *et al.* (1984)
Carbonate ion	6×10^2	PR, 11.2	Huie *et al.* (1991)
Formate ion	$<1 \times 10^6$	PR, 12	Alfassi *et al.* (1988)
tert-Butanol	$1.3 \pm 0.1 \times 10^7$ Negligible Negligible	Comp.	Wu *et al.* (2017) Kong *et al.* (2018b) Wang *et al.* (2020)
1,4-Dioxane	Negligible		Zhang *et al.* (2019)
1,1,2,3-TCBD	$3.08 \pm 0.51 \times 10^7$	Comp., 8.4	Kong *et al.* (2020a)
(*E*)-1,1,2,4-TCBD	$2.22 \pm 0.77 \times 10^7$	Comp., 8.4	Kong *et al.* (2020a)
(*Z*)-1,1,3,4-TCBD	$4.98 \pm 0.16 \times 10^7$	Comp., 8.4	Kong *et al.* (2020a)
1,1,4,4-TCBD	$2.07 \pm 0.25 \times 10^6$	Comp., 8.4	Kong *et al.* (2020a)
(*Z*,*Z*)-1,1,3,4-TCBD	$<10^6$	Comp., 8.4	Kong *et al.* (2020a)
(*Z*)-1,1,2,3,4-PCBD	$1.31 \pm 0.12 \times 10^7$	Comp., 8.4	Kong *et al.* (2020a)
1,1,2,4,4-PCBD	$1.48 \pm 0.21 \times 10^7$	Comp., 8.4	Kong *et al.* (2020a)
HCBD	$<10^6$	Comp., 8.4	Kong *et al.* (2020a)

PR, pulse radiolysis; Est., estimated; FP, flash photolysis; Comp., competitive.

6×10^2 mol^{-1} dm^3 s^{-1} (Reaction (-9), Huie *et al.* 1991). The reaction leads to an equilibrium in the electron transfer (Reactions (9) and (-9)) (Huie *et al.* 1991; Armstrong *et al.* 2015). As it was mentioned previously, the low rate constant of Reaction (-9), 6×10^2 mol^{-1} dm^3 s^{-1}, has special importance. The reactions of $^{\bullet}$OH, Cl$^{\bullet}$ and $Cl_2^{\bullet-}$ with carbonate ion (Reactions (14)–(16)) increase the importance of ClO$^{\bullet}$ reaction in the UV/chlorine process (Zhu *et al.* 2021).

Formate ions ($HCOO^-$) have low reactivity with ClO$^{\bullet}$, Alfassi *et al.* (1988) gave only an upper limit for the rate constant value, $<1 \times 10^6$ mol^{-1} dm^3 s^{-1}. Wu *et al.* (2017) using the competitive technique determined $k_{ClO^{\bullet}} = 1.3 \pm 0.1 \times 10^7$ mol^{-1} dm^3 s^{-1} for the reaction with *tert*-butanol. This rate constant value seems to be highly overestimated. Wang *et al.* (2020) reported only a minimal effect of a high concentration of *tert*-butanol on the ClO$^{\bullet}$ induced degradation of primidone. No effect of *tert*-butanol was found in the degradation of iopamidol (Kong *et al.* 2018a).

Kong *et al.* (2020a) carried out detailed investigations on the reactions of chlorinated butadienes (CBDs). In Table 2 and in Figure 1, TC refers to tetrachloro-, PC to pentachloro- and HC to hexachloro derivatives of butadiene (BD). These halogenated olefinic compounds are mainly generated during the manufacturing of chlorinated hydrocarbons. They are used as intermediates in the production of pesticides, fungicides and also have several other industrial applications. In the UV/chlorine process ClO$^{\bullet}$ was shown to be the dominant RCS in their removal. The rate constants of reactions are in the 10^7 mol^{-1} dm^3 s^{-1} range, except the reactions with (*Z,Z*)-1,2,3,4-TCBD and HCBD. The latter butadienes react with $k_{ClO^{\bullet}} < 10^6$ mol^{-1} dm^3 s^{-1}. The authors assumed that the reaction takes place by SET from HOMO of the butadienes to the LUMO of ClO$^{\bullet}$.

Benzene, substituted benzenes

The rate constants collected in Table 3, with one exception, are from the work of Li *et al.* (2021a) obtained in quantum chemical calculations (Figure 2). $k_{ClO^{\bullet}}$ values were calculated using the transition state theory (TST), they were in the 10^2–10^5 mol^{-1} dm^3 s^{-1} range. In this range it is complicated to determine $k_{ClO^{\bullet}}$ values experimentally. The value calculated by Peng *et al.* (2022) for nitrobenzene, 2.56×10^7 mol^{-1} dm^3 s^{-1}, is much higher than the value of Li *et al.* (2021a), 2.64×10^3 mol^{-1} dm^3 s^{-1}. ClO$^{\bullet}$ addition to the aromatic rings has been suggested as the main mechanism of the reaction.

Phenols and anilines

We show the compounds in these classes with published rate constants in Figure 3, a compilation of the $k_{ClO^{\bullet}}$ values is given in Table 4. The majority of rate constants here also was established in quantum chemical calculations (Li *et al.* 2021a, 2022; An *et al.* 2022) or estimated based on using the rate constants of structurally similar compounds, as well as using structure–activity relationship (QSAR) calculations (Li *et al.* 2021a; Huang & Zhang 2022). An *et al.* (2022) to establish the rate constants used TST combined with diffusion-limited effects, while Li *et al.* (2021a, 2022) used, as they said, conventional TST. The quantum chemical calculations of Li *et al.* (2021a) showed that radical adduct formation (RAF) rather than SET reaction was prominent in ClO$^{\bullet}$-initiated reactions of aromatic compounds. A similar conclusion was reported by An *et al.* (2022). In subsequent reactions of the ClO$^{\bullet}$-adduct, the Cl-end of the –OCl moiety shifted to the benzene ring, which was the key to hydroxylation and chlorination of aromatic compounds by ClO$^{\bullet}$. In contrast to the mechanism suggestions based on quantum chemical calculations, Alfassi *et al.* (1988) assumed that the basic mechanism in the reaction with phenoxides is the SET. In the reaction of the cyanophenoxide ion ($CNC_6H_4O^-$, Reaction (18)) they directly observed the formation of cyanophenoxyl

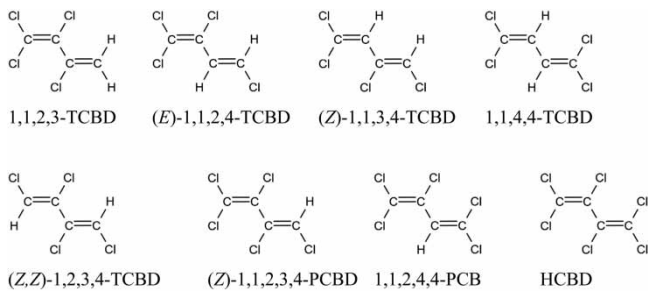

Figure 1 | Chlorinated butadienes.

Table 3 | Rate constants of benzenes

Compound	$k_{ClO•}$, $mol^{-1}\ dm^3\ s^{-1}$	Method, pH	Reference
Benzene	3.22×10^4	Calc.	Li *et al.* (2021a)
Toluene	1.56×10^4	Calc.	Li *et al.* (2021a)
Fluorobenzene	4.83×10^4	Calc.	Li *et al.* (2021a)
Chlorobenzene	4.76×10^4	Calc.	Li *et al.* (2021a)
Bromobenzene	2.37×10^4	Calc.	Li *et al.* (2021a)
Benzonitrile	2.31×10^3	Calc.	Li *et al.* (2021a)
Benzaldehyde	3.18×10^5	Calc.	Li *et al.* (2021a)
Benzamide	9.87×10^3	Calc.	Li *et al.* (2021a)
Nitrobenzene	2.64×10^3	Calc.	Li *et al.* (2021a)
	2.56×10^7	Calc., 7	Peng *et al.* (2022)
Phenylmethanol	4.06×10^6	Calc.	Li *et al.* (2021a)
Benzenesulfonic acid	4.77×10^2	Calc., neutral	Li *et al.* (2021a)
	9.99×10^3	Calc., anion	Li *et al.* (2021a)
Acetophenone	9.69×10^4	Calc.	Li *et al.* (2021a)
Benzenesulfonamide	5.04×10^2	Calc.	Li *et al.* (2021a)
Tribromomethylbenzene	3.54×10^3	Calc.	Li *et al.* (2021a)
Trichloromethylbenzene	9.13×10^3	Calc.	Li *et al.* (2021a)
Trifluoromethylbenzene	1.89×10^3	Calc.	Li *et al.* (2021a)

Calc., calculated.

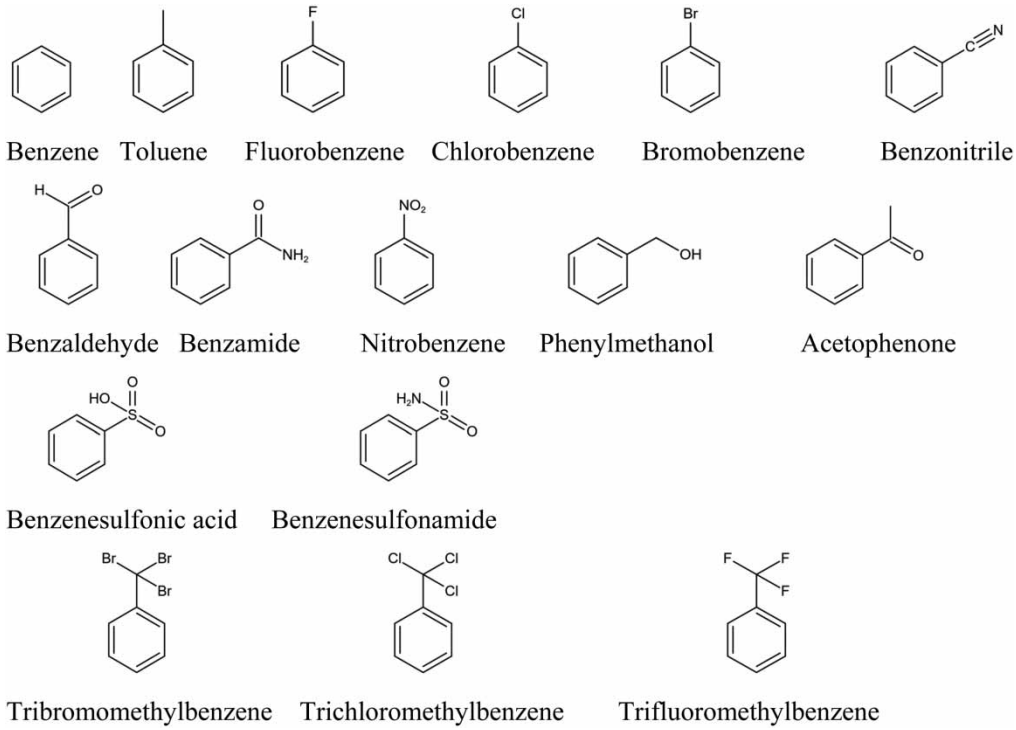

Figure 2 | Benzenes and substituted benzenes.

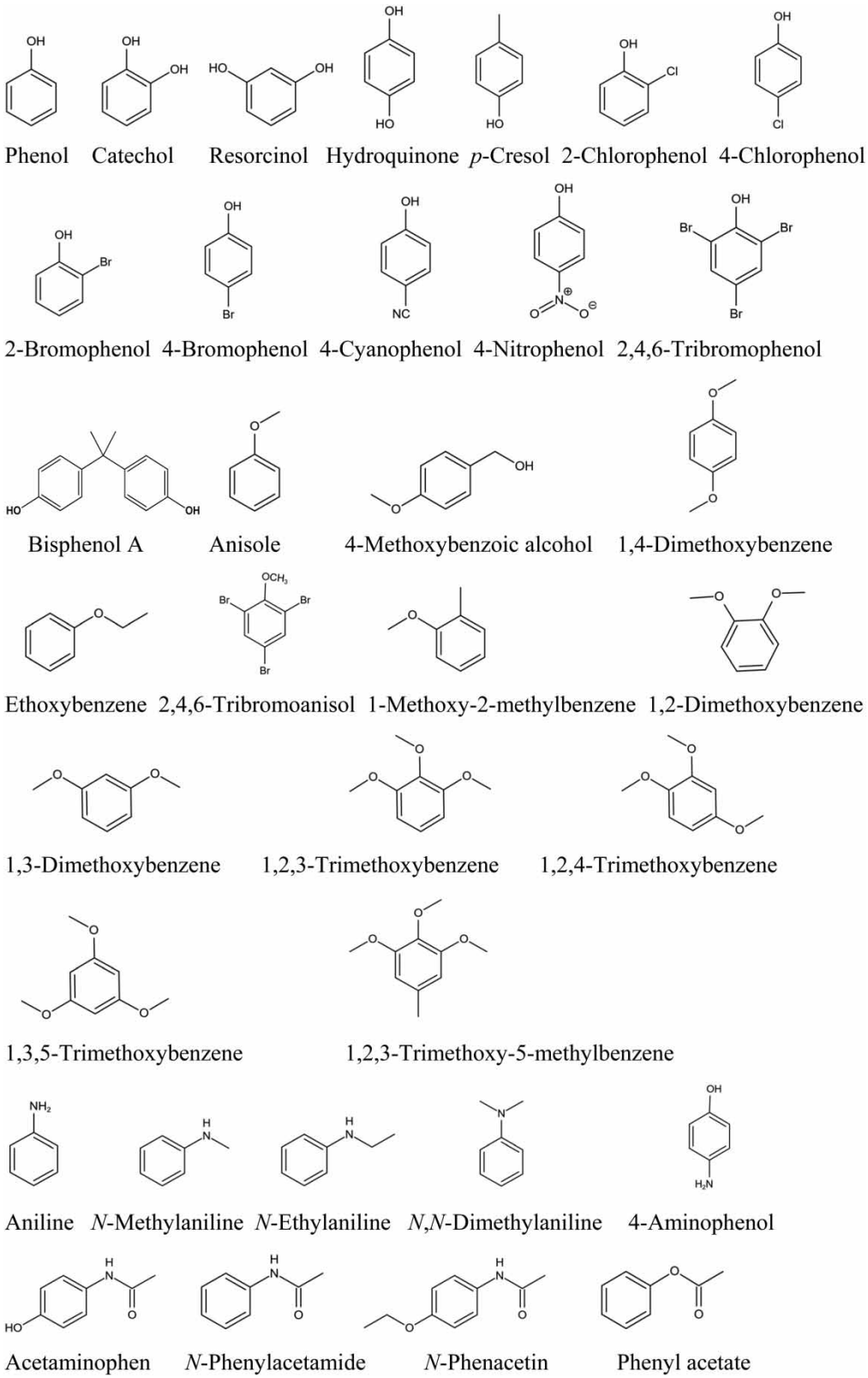

Figure 3 | Phenols and anilines.

Table 4 | Rate constants of phenols and anilines

Compound, pK_a	$k_{ClO•}$, mol^{-1} dm^3 s^{-1}	Method, pH	Reference
Phenol, 9.96	7.5×10^6	Calc., neutral	Li *et al.* (2021a)
	1.0×10^7	Est., neutral	Huang & Zhang (2022)
	6.3×10^6	Calc., neutral	An *et al.* (2022)
	2.4×10^{10}	Calc., anion	Li *et al.* (2021a)
	1.0×10^9	Est., anion	Huang & Zhang (2022)
	3.71×10^{10}	Calc., anion	An *et al.* (2022)
Catechol, 9.5	1.0×10^7	Est., neutral	Huang & Zhang (2022)
	1.0×10^9	Est., anion	Huang & Zhang (2022)
Resorcinol, 9.2	1.0×10^7	Est., neutral	Huang & Zhang (2022)
	1.0×10^9	Est., anion	Huang & Zhang (2022)
Hydroquinone, 9.9	1.0×10^7	Est., neutral	Huang & Zhang (2022)
	1.0×10^9	Est., anion	Huang & Zhang (2022)
p-Cresol, 10.36	1.55×10^6	Model., 6	Shruti Salil (2018)
2-Chlorophenol, 8.56	1.3×10^6	Est., neutral	Huang & Zhang (2022)
	1.1×10^8	Est., anion	Huang & Zhang (2022)
4-Chlorophenol, 9.2	1.3×10^6	Est., neutral	Huang & Zhang (2022)
	1.1×10^8	Est., anion	Huang & Zhang (2022)
2-Bromophenol, 8.45	1.6×10^6	Est., neutral	Huang & Zhang (2022)
	1.4×10^8	Est., anion	Huang & Zhang (2022)
4-Bromophenol, 9.17	1.6×10^6	Est., neutral	Huang & Zhang (2022)
	1.4×10^8	Est., anion	Huang & Zhang (2022)
4-Cyanophenol 8.0	1.4×10^9	PR, 13, anion	Alfassi *et al.* (1988)
4-Nitrophenol, 7.15	1.5×10^9	PR, 10, anion	Alfassi *et al.* (1988)
2,4,6-Tribromophenol, 6.8	1.9×10^5	Calc., neutral	Li *et al.* (2022)
	3.75×10^{10}	Calc., anion	Li *et al.* (2022)
Bisphenol A, 9.6	2.23×10^8	Est., 8.4	Guo *et al.* (2018)
Anisole	3.26×10^6	Calc.	Li *et al.* (2021a)
4-Methoxybenzyl alcohol	$<1.0 \times 10^7$	PR, 11	Alfassi *et al.* (1988)
1,4-Dimethoxybenzene	2.1×10^9	PR, 13	Alfassi *et al.* (1988)
	8.04×10^8	Calc.	Li *et al.* (2021a)
Ethoxybenzene	2.84×10^6	Calc.	Li *et al.* (2021a)
2,4,6-Tribromoanisol	4.26×10^4	Calc.	Li *et al.* (2022)
1-Methoxy-2-Methylbenzene	4.25×10^6	Calc.	Li *et al.* (2021a)
1,2-Dimethoxybenzene	2.41×10^8	Calc.	Li *et al.* (2021a)
1,3-Dimethoxybenzene	3.8×10^8	Calc.	Li *et al.* (2021a
1,2,3-Trimethoxybenzene	4.8×10^9	Calc.	Li *et al.* (2021a)
1,2,4-Trimethoxybenzene	1.39×10^{10}	Calc.	Li *et al.* (2021a)
1,3,5-Trimethoxybenzene	1.4×10^9	Calc.	Li *et al.* (2021a)
1,2,3-Trimethoxy-5-methylbenzene	5.47×10^9	Calc.	Li *et al.* (2021a)
Aniline, 4.63	2.07×10^3	Calc., cation	Li *et al.* (2021a)
	1.11×10^{10}	Calc., neutral	Li *et al.* (2021a)
	3.28×10^5	Calc., cation	An *et al.* (2022)
	1.47×10^{10}	Calc., neutral	An *et al.* (2022)
p-Aminophenol, 5.4, 9.9	8.05×10^5	Calc., cation	An *et al.* (2022)
	5.35×10^{10}	Calc., anion	An *et al.* (2022)
N,*N*-Dimethylaniline, 5.15	1.81×10^{10}	Calc.	Li *et al.* (2021a)
N-Ethylaniline, 5.12	2.66×10^{10}	Calc.	Li *et al.* (2021a)

(*Continued.*)

Table 4 | Continued

Compound, pK_a	$k_{ClO^{\bullet}}$, mol^{-1} dm^3 s^{-1}	Method, pH	Reference
N-Methylaniline, 4.85	2.49×10^{10}	Calc.	Li *et al.* (2021a)
N-Phenylacetamide	1.8×10^{7}	Calc.	Li *et al.* (2021a)
Phenacetin	2.13×10^{8}	Calc.	Li *et al.* (2021a)
Phenyl acetate	1.32×10^{4}	Calc.	Li *et al.* (2021a)
Acetaminophen (paracetamol), 9.4	3.53×10^{9}	Comp., 8.5	Giang *et al.* (2017)
	4.61×10^{8}	Calc., neutral	Li *et al.* (2021a)
	7.74×10^{6}	Calc., neutral	Wang *et al.* (2021b)

Calc., calculated; Est., estimated; Model., modeling; PR, pulse radiolysis; Comp., competitive.

radical ($CNC_6H_4O^{\bullet}$) in pulse radiolysis experiments.

$$CNC_6H_4O^- + ClO^{\bullet} \rightarrow CNC_6H_4O^{\bullet} + ClO^- \quad (18)$$

The calculated $k_{ClO^{\bullet}}$ value of 1,4-dimethoxybenzene (8.04×10^8 mol^{-1} dm^3 s^{-1}, Li *et al.* 2021a) was found to be smaller than the experimental rate constant (2.1×10^9 mol^{-1} dm^3 s^{-1}) of Alfassi *et al.* (1988). The calculated $ClO^{\bullet}$ initiated reaction rate constants of aromatic compounds are in the range of 10^2–10^{10} mol^{-1} dm^3 s^{-1}. $ClO^{\bullet}$ was found to be highly reactive to phenolates, anilines and alkoxy/hydroxyl aromatic compounds. Upon the deprotonation of phenol to phenolate, the $k_{ClO^{\bullet}}$ value increased by four orders of magnitude, from 6.3×10^6–1×10^7 mol^{-1} dm^3 s^{-1} to 1×10^9–3.71×10^{10} mol^{-1} dm^3 s^{-1} (Li *et al.* 2021a; An *et al.* 2022; Huang & Zhang 2022). (The latter value seems to be unrealistic since it is much higher than the diffusion-limited rate constant of $\sim 1 \times 10^{10}$ mol^{-1} dm^3 s^{-1} (Kovács *et al.* 2022).) The deprotonation of the phenolic OH resulted in the sudden increase of the rate constant in the reactions of a number of other phenol type compounds as shown in Table 4. E.g., in the case of 2,4,6-tribromophenol $k_{ClO^{\bullet}}$ increased from 1.95×10^5 to 3.71×10^{10} mol^{-1} dm^3 s^{-1} (Li *et al.* 2022). The $k_{ClO^{\bullet}}$ values of alkoxybenzenes are higher for compounds with shorter alkyl side chains and more alkoxy substituents.

Due to the electrophile character of $k_{ClO^{\bullet}}$ reactions the calculated rate constants highly increase upon deprotonation of aniline cation. Li *et al.* (2021a) calculated values of 2.07×10^3 and 1.11×10^{10} mol^{-1} dm^3 s^{-1} for aniline cation and the neutral molecule, respectively. The calculated values of An *et al.* (2022) are closer to each other: 3.28×10^5 and 1.47×10^{10} mol^{-1} dm^3 s^{-1}, respectively.

p-Aminophenol has two dissociable places, the amino group and the hydroxyl group. In the pH range between 0 and 14, the ionization state changes in the order: cation, neutral, zwitterion and anion. The calculated rate constants gradually increase with the pH. For *p*-aminophenol cation and anion, An *et al.* (2022) calculated $k_{ClO^{\bullet}}$ values of 8.05×10^5 and 5.35×10^{10} mol^{-1} dm^3 s^{-1}, respectively, the rate constant of the neutral species lies between the two. Acetaminophen (paracetamol, used as a non-steroidal anti-inflammatory drug, NSAID) is a derivative of *p*-aminophenol. Giang *et al.* (2017) by using the competitive technique published $k_{ClO^{\bullet}} = 3.53 \times 10^9$ mol^{-1} dm^3 s^{-1}, while the theoretical calculations of Li *et al.* (2021a) and Wang *et al.* (2021b) based on the TST yielded one and three orders of magnitude smaller values: 4.61×10^8 and 7.74×10^6 mol^{-1} dm^3 s^{-1}, respectively. The chemical structure of *N*-phenacetin (*N*-(4-ethoxyphenyl)acetamide, also used as NSAID) is similar to that of acetaminophenen. The calculated rate constant values for the two medicines, for the neutral acetaminophen and phenacetin (Li *et al.* 2021a) are also close to each other.

Benzoic acid and derivatives

In Table 5, the rate constant values for benzoic acids taken from the works of Li *et al.* (2021a), An *et al.* (2022) and Peng *et al.* (2022) were obtained in quantum chemical calculations using the TST. The values of Zhou *et al.* (2019) were estimated through a complex fitting procedure to the concentration changes of the compound investigated in UV/chlorine process. Only the values of Alfassi *et al.* (1988) were obtained in direct pulse radiolysis experiments. The latter authors for the $k_{ClO^{\bullet}}$ of the benzoate ion gave an upper limit of $<3.0 \times 10^6$ mol^{-1} dm^3 s^{-1}. The calculated rate constant of An *et al.* (2022), 8.88×10^4 mol^{-1} dm^3 s^{-1}, and that of Li *et al.* (2021a), 6.68×10^4 mol^{-1} dm^3 s^{-1} are also very low. Peng *et al.* (2022) calculated three orders of magnitude higher value for the anion: 2.32×10^7 mol^{-1} dm^3 s^{-1}. The values given for the neutral molecule, 7.26×10^3 and 3.13×10^3 mol^{-1} dm^3 s^{-1}, published by Li *et al.* (2021a) and An *et al.* (2022), respectively, are much smaller than the values for the anion.

Table 5 | Benzoic acid and derivatives

Compound, pK_a	$k_{ClO^•}$, mol^{-1} dm^3 s^{-1}	Method, pH	Reference
Benzoic acid, 4.2	7.26×10^3	Calc., neutral	Li *et al.* (2021a)
	3.13×10^3	Calc., neutral	An *et al.* (2022)
	$<3.0 \times 10^6$	PR, 12, anion	Alfassi *et al.* (1988)
	6.68×10^4	Calc., anion	Li *et al.* (2021a)
	2.32×10^7	Calc., 7	Peng *et al.* (2022)
	8.88×10^4	Calc., anion	An *et al.* (2022)
Methylbenzoate	1.02×10^4	Calc., anion	Li *et al.* (2021a)
3-Methylbenzoic acid, 4.27	1.21×10^6	Est., 7.2, anion	Zhou *et al.* (2019)
4-Fluorobenzoic acid, 4.14	1.27×10^6	Est., 7.2, anion	Zhou *et al.* (2019)
2-Chlorobenzoic acid, 2.9	8.00×10^5	Est., 7.2, anion	Zhou *et al.* (2019)
4-Chlorobenzoic acid, 3.98	3.13×10^7	Calc., anion	Peng *et al.* (2022)
2-Iodobenzoic acid, 2.86	8.82×10^5	Est., 7.2, anion	Zhou *et al.* (2019)
3-Cyanobenzoic acid, 3.6	8.11×10^5	Est., 7.2, anion	Zhou *et al.* (2019)
3-Nitrobenzoic acid, 3.4	5.05×10^5	Est., 7.2, anion	Zhou *et al.* (2019)
p-Hydroxybenzoic acid, 4.38, 9.3	7.05×10^4	Calc., neutral	An *et al.* (2022)
	3.7×10^{10}	Calc., dianion	An *et al.* (2022)
p-Aminobenzoic acid, 2.38, 4.85	2.78×10^5	Calc., cation	An *et al.* (2022)
	7.62×10^9	Calc., anion	An *et al.* (2022)
2,4,5-Trimethoxybenzoic acid, 4.24	1.1×10^9	PR, 13, anion	Alfassi *et al.* (1988)
	1.62×10^{10}	Calc., anion	Li *et al.* (2021a)
2,5-Dimethoxybenzoic acid, 3.97	7.0×10^8	PR, 13, anion	Alfassi *et al.* (1988)
	4.11×10^9	Calc., anion	Li *et al.* (2021a)

Calc., calculated; PR, pulse radiolysis; Est., estimated.

Both experimentally (pulse radiolysis) determined (1.1×10^9 and 7.0×10^8 mol^{-1} dm^3 s^{-1}, Alfassi *et al.* 1988) and calculated rate constants (1.62×10^{10} and 4.11×10^9 mol^{-1} dm^3 s^{-1}, Li *et al.* 2021a) are also available for 2,4,5-trimethoxybenzoate and 2,4-dimethoxybenzoate, respectively (Figure 4). The values obtained by the two methods differ by one order of magnitude. Li *et al.* (2021a) mentions that the experimental values were obtained with a single technique, and other experimental methods should be used to determine $k_{ClO^•}$ values. We mention here that often for the same compound, several quantum chemical calculations were carried out in different laboratories, the results usually differ also by at least one order of magnitude.

As the calculated results for *p*-hydroxybenzoic acid and *p*-aminobenzoic acid show, similarly to benzoic acid, deprotonation, and thereby the increase of electron density on the benzene ring greatly increases the rate constant. According to the estimations of Zhou *et al.* (2019) electron donating substituents on the ring of benzoate increase, electron-withdrawing substituents decrease the rate constants.

Li *et al.* (2021a) mention that $ClO^•$ reactions likely to play an important role in the UV/chlorine process when $k_{ClO^•}$ is greater than 10^6 mol^{-1} dm^3 s^{-1}. The $k_{ClO^•}$ values of many aromatic compounds were found above this limit: the order was: anilines ≈ phenolate > trimethoxy-benzenes > dimethoxybenzenes > phenylamides > phenol > phenylmethanol > mono-alkoxybenzenes. Among these, the $k_{ClO^•}$ values of anilines, phenolate, dimethoxy- and trimethoxy-benzenes were greater than 10^8 mol^{-1} dm^3 s^{-1}.

Pharmaceuticals and related compounds

The synthetic nitroimidazole antibiotics, metronidazole, dimetridazole, ornidazole, ronidazole and tinidazole are used in form of tablets, in creams and in injection (Figure 5). Guo *et al.* (2018) in competitive experiments for dimetridazole, ornidazole, ronidazole and tinidazole established rate constants in the range 1.37×10^6–1.1×10^7 mol^{-1} dm^3 s^{-1}. Wu *et al.* (2017) based on competitive experiments for metronidazole gave a value of $<1 \times 10^6$ mol^{-1} dm^3 s^{-1} (Table 6). Guo *et al.* (2018) noticed that $ClO^•$ prefers to react with electron-rich molecules or electron-rich molecular parts. The natural logarithms

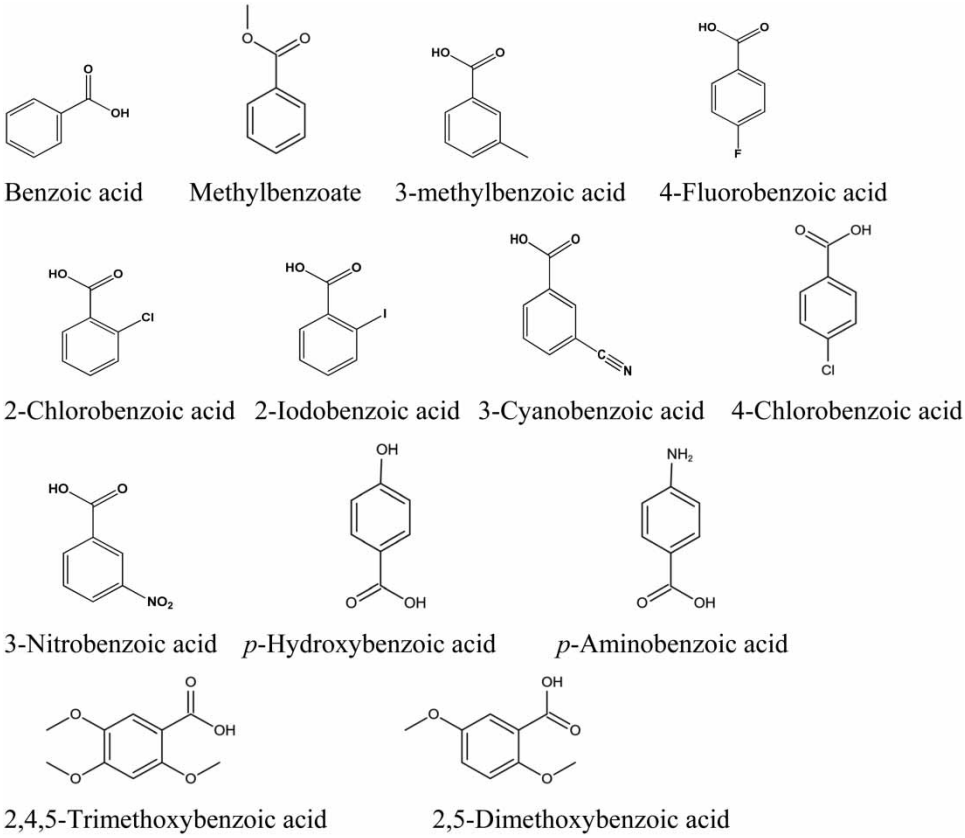

Figure 4 | Benzoic acid and derivatives.

of rate constant values of 16 compounds, among them those of nitroimidazoles showed a good correlation with the Hammett σ^+ substituent constants: $\ln k_{ClO^\bullet} = -3.6\ \Sigma\ \sigma^+ + 15.4$.

Erythromicin is an often applied macrolide-type antibiotic. Kim *et al.* (2020) investigated the pH dependence of its reaction with $ClO^\bullet$. The rate constant increased in the pH range 6–10 from 3.1×10^9 to 1×10^{10} mol^{-1} dm^3 s^{-1}, due to deprotonation with pK_a 8.9. The authors established that in the UV-LED(275 nm)/chlorine process at high pH the $Cl^\bullet$ and $ClO^\bullet$ radicals played the key role in the degradation.

Wang *et al.* (2021a) carried out pH dependence studies on the reaction of trimethoprim. This medicine is often used in combination with sulfa drugs, e.g., sulfamethoxazole or sulfadiazine. At low pH both N-atoms in the heterocyclic ring are protonated, at high pH the neutral form dominates (pK_{a1} 3.1, pK_{a2} 7.1). Under the usual conditions there is a pH determined equilibrium between the dication ($Trim^{2+}$), the monocation ($Trim^+$) and the neutral forms. From the fitted results of Wang *et al.* (2021a) it seems that the neutral form has the smallest rate constant, 1.93×10^6 mol^{-1} dm^3 s^{-1}. The rate constant of Guo *et al.* (2018) predicted for the $ClO^\bullet$ + trimethoprim reaction, 4.46×10^{10} mol^{-1} dm^3 s^{-1}, is out of the range of rate constants of chlorine monoxide reactions shown in the tables in this paper.

Both 2-phenylbenzimidazole-5-sulfonic acid (PBSA) and sulfamethoxazole are derivatives of sulfonic acid. PBSA as a personal care product (PCP) is used as an organic filter of UV radiation. Therefore, its concentration is often high in swimming pools and recreation waters, it appears also in lakes and rivers. In swimming pools usually, chlorination is used for disinfection. Therefore, under the effect UV light in open-air swimming pools PBSA is attacked by different chlorine radicals, among them $ClO^\bullet$. Yin *et al.* (2022) using competitive experiments published a rate constant of 1.5×10^5 mol^{-1} dm^3 s^{-1}. Based on similar experiments the $k_{ClO^\bullet}$ value of Hu *et al.* (2022) is 8.6×10^7 mol^{-1} dm^3 s^{-1}. Considering the rate constants of similar compounds, we tend to believe that the $k_{ClO^\bullet}$ value of Yin *et al.* (2022) is closer to reality than the rate constant of Hu *et al.* For sulfamethoxazole (antibiotic), Guo *et al.* (2018) calculated an unrealistically high upper limit for the rate constant: $<2.23 \times 10^9$ mol^{-1} dm^3 s^{-1}. Zheng *et al.* (2022) suggested that rate constant of sulfamethoxazole is very low; they observed very slow degradation of the target compound when the $ClO^\bullet$ dominated in the reaction mixture.

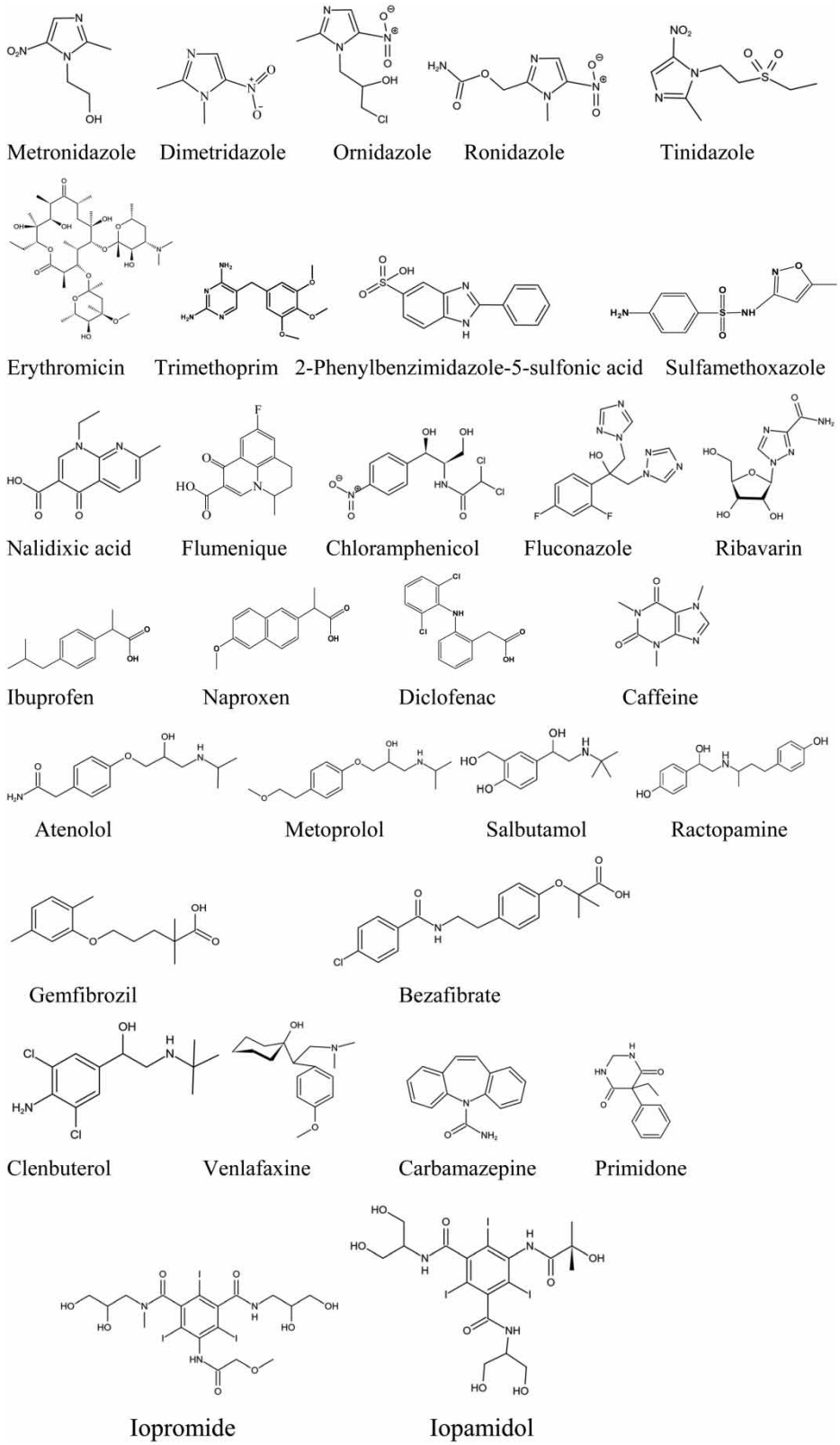

Figure 5 | Pharmaceuticals and related compounds.

Table 6 | Pharmaceuticals and related compounds

Compound, pK_a	$k_{ClO•}$, $mol^{-1}\ dm^3\ s^{-1}$	Method, pH	Reference
Metronidazole, 2.57	$<1.0 \times 10^6$	Comp., 7	Wu *et al.* (2017)
	$<1.0 \times 10^4$	Comp., 7.2	Wang *et al.* (2022a)
Dimetridazole	1.1×10^7	Comp., 8.4	Guo *et al.* (2018)
Ornidazole	4.12×10^6	Comp., 8.4	Guo *et al.* (2018)
Ronidazole	5.49×10^6	Comp., 8.4	Guo *et al.* (2018)
Tinidazole	1.37×10^6	Comp., 8.4	Guo *et al.* (2018)
Erythromicin, 8.9	3.1×10^9	Comp., 6	Kim *et al.* (2020)
	3.3×10^9	Comp., 7	Kim *et al.* (2020)
	7.5×10^9	Comp., 8	Kim *et al.* (2020)
	1×10^{10}	Comp., 9	Kim *et al.* (2020)
Trimethoprim, 3.1, 7.1	4.46×10^{10}	Pred., 8.4	Guo *et al.* (2018)
	2.1×10^9		Teo *et al.* (2022)
	9.2×10^6	Fit., dianion	Wang *et al.* (2021a)
	2.77×10^6	Fit., monoanion	
	1.93×10^6	Fit., neutral	
2-Phenylbenzimidazole-5-sulfonic acid, -0,87	1.5×10^5	Comp. 8.4	Yin *et al.* (2022)
	8.6×10^7	Comp, 7	Hu *et al.* (2022)
Sulfamethoxazole, 1.6, 5.7	$<2.23 \times 10^9$	Comp., 8.4	Guo *et al.* (2018)
	negligible		Zheng *et al.* (2022)
Nalidixic acid, 5.95	$<8.9 \times 10^6$	Comp., 7	Wu *et al.* (2017)
	1.79×10^7	Comp., 8.4	Guo *et al.* (2018)
Flumenique	2.75×10^7	Comp., 8.4	Guo *et al.* (2018)
Chloramphenicol	negligible	Comp., 8.4	Guo *et al.* (2018)
Fluconazole, 2.27	4.0×10^7	Comp., 7	Cai *et al.* (2020)
	9.48×10^7	Calc.	
Ribavarin	5.58×10^7	Comp., 8.4	Sun *et al.* (2022)
Ibuprofen, 4.9	5.49×10^6	Comp., 8.4	Guo *et al.* (2018)
Naproxen, 4.2	$<5.69 \pm 0.36 \times 10^9$	Comp., 7	Pan *et al.* (2018)
	$<2.3 \times 10^9$	Comp., 8.4	Guo *et al.* (2018)
	9.24×10^9	Comp. 8.4	Liu *et al.* (2021)
Diclofenac, 4.2	3.54×10^8	Pred., 8.4	Guo *et al.* (2018)
Caffeine	1.4×10^3	Est.	Sun *et al.* (2016)
	1.03×10^8	Comp, 8.4.	Guo *et al.* (2017)
	$5.1 \pm 0.2 \times 10^7$	Comp., 7	Wu *et al.* (2017)
	1.31×10^8	Comp., 8.4	Guo *et al.* (2018)
	1.4×10^9	Calc.	Li *et al.* (2021b)
Atenolol, 9.5	8.68×10^7	Comp., 8.4	Guo *et al.* (2018)
Metoprolol, 9.6	1.34×10^8	Comp., 8.4	Guo *et al.* (2018)
Salbutamol, 10.12	1.21×10^8	Pred., 8.4	Guo *et al.* (2018)
Ractopamine, 9.4	8.59×10^9	Pred., 8.4	Guo *et al.* (2018)
Gemfibrozil, 4.5	$4.2 \pm 0.3 \times 10^8$	Comp., 8.4	Kong *et al.* (2018b)
	4.16×10^8	Comp., 8.4	Guo *et al.* (2017)
	4.16×10^8	Comp., 8.4	Guo *et al.* (2018)
	1.93×10^9	Comp., 8.4	Liu *et al.* (2021)
Bezafibrate, 3.83	$3.6 \pm 0.1 \times 10^7$	Comp., 8.4	Kong *et al.* (2018b)
	5.0×10^8	Model.	Shi *et al.* (2018)
Clenbuterol	$<5.0 \times 10^9$	Comp., 8.4	Guo *et al.* (2018)
Venlafaxine	1.65×10^8	Comp., 8.4	Guo *et al.* (2018)

(*Continued.*)

Table 6 | Continued

Compound, pK_a	$k_{ClO^{\bullet}}$, $mol^{-1}\ dm^3\ s^{-1}$	Method, pH	Reference
Carbamazepine, 13.9	9.2×10^7	Comp., 8.4	Guo *et al.* (2017)
	1.97×10^8	Comp., 8.4	Guo *et al.* (2018)
	1.78×10^6	Fit., 7	Zhu *et al.* (2021)
	$1.21 \pm 0.08 \times 10^7$	Fit.	Zhang *et al.* (2022)
Primidone, 12.3	5.51×10^7	Comp., 8.4	Guo *et al.* (2018)
	1.12×10^6	Simul., 8.4	Wang *et al.* (2020)
Iopromide, 9.9	1.25×10^9	Comp., 7	Cha *et al.* (2022)
Iopamidol	7.3×10^7	Comp., 10	Luo *et al.* (2022)

Comp., competitive; Pred., predicted; Fit., fitting; Calc., calculated; Est., estimated; Model., modeling; Simul., simulating.

Nalidixic acid is a narrow-spectrum antibacterial agent used for treating urinary tract infections. The second-order rate constant of reaction with $ClO^{\bullet}$ is published as $<8.9 \times 10^6\ mol^{-1}\ dm^3\ s^{-1}$ (Wu *et al.* 2017) and $1.79 \times 10^7\ mol^{-1}\ dm^3\ s^{-1}$ (Guo *et al.* 2018). The chemical structure of nalidixic acid reminisces that of the fluoroquinolone antibiotics, e.g., that of flumenique. The rate constant of the latter compound was published as $2.75 \times 10^7\ mol^{-1}\ dm^3\ s^{-1}$ (Guo *et al.* 2018). Chloramphenicol is effective against a wide variety of microorganisms, but due to serious side-effects in humans, it is usually reserved for the treatment of serious and life-threatening infections (e.g., typhoid fever). It is rather inactive in reaction with $ClO^{\bullet}$ due to the electron-withdrawing nitro group and the chlorine atoms in the molecule (Guo *et al.* 2018).

Fluconazole (medicine used to treat fungal infections) has two triazole rings. Radical addition is suggested as the main reaction of $ClO^{\bullet}$ with fluconazole (Cai *et al.* 2020). The experimentally obtained rate constant is $4.0 \times 10^7\ mol^{-1}\ dm^3\ s^{-1}$, the value obtained by DFT calculations, $9.48 \times 10^7\ mol^{-1}\ dm^3\ s^{-1}$ is two times higher than the experimental one. There is another medicine, ribavirin, in Table 6 with a triazole ring. Ribavarin is an antiviral agent that is used, for instance, to treat hepatitis C. The rate constant obtained in competitive experiments ($5.58 \times 10^7\ mol^{-1}\ dm^3\ s^{-1}$, Sun *et al.* 2022) is close to the value published for fluconazole.

Ibuprofen and naproxen are propionic acid-based non-steroidal anti-inflammatory drugs (NSAIDs). The rate constant of $ClO^{\bullet}$ reaction with ibuprofen based on competitive experiments was published as $5.49 \times 10^6\ mol^{-1}\ dm^3\ s^{-1}$ (Guo *et al.* 2018). For naproxen, competitive experiments in three laboratories suggest $k_{ClO^{\bullet}}$ values in the $10^9\ mol^{-1}\ dm^3\ s^{-1}$ order of magnitude range (Guo *et al.* 2018; Pan *et al.* 2018; Liu *et al.* 2021). The three orders of magnitude higher value for naproxen than for ibuprofen is certainly due to the naphthalene unit in the molecule which offers an excellent possibility for electrophile attack. An increase in the rate constant upon replacing benzene with the naphthalene unit caused an increase also in the rate constants of reactions of other one-electron oxidants, e.g., in the reactions of β-blockers (Kovács *et al.* 2022). Diclofenac is also an NSAID. In the molecule, an amino group connects two aromatic rings. The $k_{ClO^{\bullet}}$ value predicted for this medicine (Guo *et al.* 2018), $3.54 \times 10^8\ mol^{-1}\ dm^3\ s^{-1}$, is similar to those of rate constants given for compounds with two aromatic rings.

The $k_{ClO^{\bullet}}$ value of caffeine reaction with $ClO^{\bullet}$ was published in several papers. Actually, caffeine often served as a model compound in investigations of the UV/chlorine process. The published rate constants range from the value estimated based on structure-reactivity relations, $1.4 \times 10^3\ mol^{-1}\ dm^3\ s^{-1}$ (Sun *et al.* 2016) to the calculated value (quantum chemistry) of Li *et al.* (2021b), $1.4 \times 10^9\ mol^{-1}\ dm^3\ s^{-1}$. The experimentally obtained values are around $1 \times 10^8\ mol^{-1}\ dm^3\ s^{-1}$ (Guo *et al.* 2017, 2018; Wu *et al.* 2017). Theoretical calculations showed that the basic reaction is $ClO^{\bullet}$-adduct formation, just like in the cases of $^{\bullet}OH$ and $BrO^{\bullet}$ reactions (Li *et al.* 2021a).

Atenolol, metoprolol, salbutamol and ractopamine as β-blockers are used to treat cardiovascular diseases. These compounds are propionamide derivatives, all containing benzene or naphthalene unit. There are two main vulnerable sites for a radical attack in these molecules, the aromatic ring(s) and the amino group (Kovács *et al.* 2022). Guo *et al.* (2018) in competitive experiments determined rate constants of 8.68×10^7 and $1.34 \times 10^8\ mol^{-1}\ dm^3\ s^{-1}$, respectively, for atenolol and metoprolol. They predicted $k_{ClO^{\bullet}}$ values of 1.21×10^8 and $8.59 \times 10^9\ mol^{-1}\ dm^3\ s^{-1}$ for salbutamol and ractopamine, respectively. The high value of the latter may be rationalized by the two aromatic rings in the molecule. Both rings have electron releasing hydroxyl group in *para* position.

In the literature, we found four values for the $k_{ClO^{\bullet}}$ of gemfibrozil reaction (a medicine used to regulate blood lipid level). All values were established in competitive experiments. The values of Guo *et al.* (2017, 2018) and Kong *et al.* (2018b) are ~ 4.2×10^8 mol^{-1} dm^3 s^{-1}, Liu *et al.* (2021) published higher value: 1.93×10^9 mol^{-1} dm^3 s^{-1}. Bezafibrate is also used to control lipid levels in the blood. The rate constants published by Kong *et al.* (2018b) and Shi *et al.* (2018) differ by one order of magnitude, $3.6 \pm 0.1 \times 10^7$ and 5.0×10^8 mol^{-1} dm^3 s^{-1}, respectively. Kong *et al.* (2018b) used competitive experiments, while Shi *et al.* (2018) applied modeling calculations in the UV/chlorine process.

In clenbuterol (veterinary drug) a similar side chain is attached to the aromatic ring as in salbutamol. There are two chlorine atoms and an amine group in the ring. Guo *et al.* (2018) gave a surprisingly high upper limit for the rate constant: $<5.0 \times 10^9$ mol^{-1} dm^3 s^{-1}. Because of the two electron-withdrawing Cl atoms on the ring, we expect a much smaller rate constant. The antidepressant medicine venlafaxine, similar to the β-blockers has also an aromatic ring and in the side chain a tertiary amine group. The rate constant is in the 10^8 mol^{-1} dm^3 s^{-1} order of magnitude range as those of the β-blockers (Guo *et al.* 2018).

Carbamazepine is used as an anticonvulsant or anti-epileptic drug. Guo *et al.* (2017, 2018) in two papers published two different rate constants based on competitive experiments, although the values are not very far from each other, 9.7×10^7 and 1.97×10^8 mol^{-1} dm^3 s^{-1}. The value of Zhu *et al.* (2021) obtained in UV/chlorine experiments, by using complex fitting procedure, 1.78×10^6 mol^{-1} dm^3 s^{-1}, is two orders of magnitude smaller than the values of Guo *et al.* (2017, 2018). Primidone in the medical practice is also used to treat epilepsy. Guo *et al.* (2018) in competitive experiments determined a value of 5.51×10^7 mol^{-1} dm^3 s^{-1}, while Wang *et al.* (2020) in simulation experiments estimated an order of magnitude smaller rate constant, 1.12×10^6 mol^{-1} dm^3 s^{-1}.

Iopromide and iopamidol have similar structures, in both of them there is a central benzene ring with three iodine atoms. Due to the iodine heavy atoms, they are used as X-ray contrast media in organ imaging. Their $k_{ClO^{\bullet}}$ values were established in competitive experiments and they differ by a factor of 17: 1.25×10^9 and 7.3×10^7 mol^{-1} dm^3 s^{-1}, respectively (Cha *et al.* 2022; Luo *et al.* 2022). It is hard to say the reason for this large difference, in spite of the similar structure. The different pH values applied during the measurements (pH 7 and 10) may influence $k_{ClO^{\bullet}}$. In UV/chlorine degradation of both contrast materials $ClO^{\bullet}$ reaction has the dominant role (Kong *et al.* 2018a).

Miscellaneous compounds

Synthetic musks are chemicals that are used in many cosmetic products, among others in deodorants and detergents (Table 7, Figure 6). Some of them show toxic effects in the aquatic environment. We found experimentally determined rate constant value only for acetyl hexamethyl tetralin (AHTN, called also musk tonalide). The value determined in the competitive experiments of Wang & Liu (2019), 6.3×10^9 mol^{-1} dm^3 s^{-1}, is higher than the value, 1.1×10^7 mol^{-1} dm^3 s^{-1}, predicted for this compound and the other synthetic aromatic musks (HHCB, ADBI, ATII, AHMI, MK, 4.6×10^4–6.8×10^7 mol^{-1} dm^3 s^{-1}, Table 7) by Lee *et al.* (2022) based on the QSAR equation of Guo *et al.* (2018) for $ClO^{\bullet}$ reactions ($k_{ClO^{\bullet}} = -3.5\ \Sigma\ \sigma^+ + 15.4$). For the three olefinic musks in Table 7 (OTNE, ABMT, DPMI), Lee *et al.* (2022) assumed 2.5×10^7 mol^{-1} dm^3 s^{-1} based on the reactivity of $ClO^{\bullet}$ toward olefin compounds (CBDs) observed by Kong *et al.* (2020a). $ClO^{\bullet}$ is suggested to have a determining role in the degradation of synthetic musks in the UV/Chlorine process. Geosmin, a natural fragrance, is a bicyclic alcohol, a derivative of decalin. It gives the taste and odour of drinking water. The compound has low reactivity with all chlorine radicals (Fang *et al.* 2018).

Clothianidin (used as insecticide) contains a 5-member thiazole ring. The rate constant established in competitive experiments seems to be overestimated: $7.3 \pm 0.1 \times 10^9$ mol^{-1} dm^3 s^{-1} (Lee *et al.* 2021). It is 4.3 times higher than the rate constant of $^{\bullet}OH$ reaction: $1.7 \pm 0.2 \times 10^9$ mol^{-1} dm^3 s^{-1}. $ClO^{\bullet}$ is suggested to attack the C-atom on the C = N moiety to substitute the nitroamino moiety of the urea compound. Benzothiazoles and benzotriazoles have also 5-member haterocyclic rings. They are widely applied in various consumer and industrial products, e.g., as vulcanization additives in rubber industry or as corrosion inhibitors. Yang *et al.* (2021) using radical scavengers in the UV/chlorine process derived similar second-order rate constants for the $ClO^{\bullet}$ reaction of benzothiazole and benzotriazole: 2.22×10^8 and 2.4×10^8 mol^{-1} dm^3 s^{-1}, respectively. Choo *et al.* (2022) measured an increase in the rate constant for benzotriazole from $1.46 \pm 0.09 \times 10^8$ to $2.1 \pm 0.1 \times 10^8$ mol^{-1} dm^3 s^{-1} as the pH increased from 8.4 to 8.8, the pK_a is at 8.3. These $k_{ClO^{\bullet}}$ values are much smaller than the rate constant published for clothianidin (Lee *et al.* 2021).

N,*N*-Diethyl-*meta*-toluamide (DEET) is used as an insect repellent. It is rather inert in reaction with $ClO^{\bullet}$: $k_{ClO^{\bullet}} < 1.0 \times 10^6$ mol^{-1} dm^3 s^{-1} (Wu *et al.* 2017). The chlorophenoxy type herbicide mecoprop is widely used even now for weed control,

Table 7 | Miscellaneous compounds

Compound, pK_a	$k_{ClO^{\bullet}}$, $mol^{-1}\ dm^3\ s^{-1}$	Method, pH	Reference
Acetyl hexamethyl tetralin (AHTN)	6.3×10^9	Comp. 8.4	Wang & Liu (2019)
	1.1×10^7	Pred.	Lee *et al.* (2022)
Hexahydro hexamethyl cyclopentabenzopyran (HHCB)	6.8×10^7	Pred.	Lee *et al.* (2022)
Acetyl dimethyl tert-butyl indane (ADBI)	9.8×10^6	Pred.	Lee *et al.* (2022)
Acetyl tetramethyl isopropyl indane (ATII)	1.2×10^7	Pred.	Lee *et al.* (2022)
Acetyl hexamethyl indane (AHMI)	1.1×10^7	Pred.	Lee *et al.* (2022)
Musk ketone (MK)	4.6×10^4	Pred.	Lee *et al.* (2022)
Octahydro tetramethyl naphthalenyl ethanone (OTNE)	2.5×10^7	Assum.	Lee *et al.* (2022)
Ambrettolide (AMBT)	2.5×10^7	Assum.	Lee *et al.* (2022)
Dihydro pentamethyl indanone (DPMI)	2.5×10^7	Assum.	Lee *et al.* (2022)
Geosmin	Negligible		Fang *et al.* (2018)
Clothianidin, 11.09	$7.3 \pm 0.1 \times 10^9$	Comp., 8.4	Lee *et al.* (2021)
Benzotriazole, 8.3	2.4×10^8	Model., 7	Yang *et al.* (2021)
	$1.46 \pm 0.09 \times 10^8$	Comp., 8.4	Choo *et al.* (2022)
	$1.93 \pm 0.12 \times 10^8$	Comp., 8.65	
	$2.1 \pm 0.1 \times 10^8$	Comp., 8.8	
Benzothiazole, 2.28	2.22×10^8	Model., 7	Yang *et al.* (2021)
Diethyltoluamide (DEET)	$<1.0 \times 10^6$	Comp., 7	Wu *et al.* (2017)
Mecoprop	1.11×10^8	Comp., 7	Kong *et al.* (2020b)
Atrazine	$<1 \times 10^6$	Comp.	Kong *et al.* (2020b)
	Negligible		Ye *et al.* (2021)
NOM	$4.5 \times 10^4\ mgC^{-1}\ dm^3\ s^{-1}$	Model., 8.4	Guo *et al.* (2017)

Comp., competitive; Pred., predicted; Assum., assumed; Model., modeling.

while the other herbicide atrazine, often used in the past, is banned in many countries. In the UV/chlorine process, mecoprop decomposes to a large extent in $ClO^{\bullet}$ reactions ($k_{ClO^{\bullet}} = 1.11 \times 10^8\ mol^{-1}\ dm^3\ s^{-1}$, Kong *et al.* 2020b). At the same time, atrazine is rather unreactive in reaction with this radical ($<10^6\ mol^{-1}\ dm^3\ s^{-1}$ (Kong *et al.* 2020b; Ye *et al.* 2021)). Contrary to this statement, in the bisulfite/chlorine dioxide system $ClO^{\bullet}$and $SO_4^{\bullet-}$ were suggested as the main radical intermediates that destroy atrazine (Wang *et al.* 2022b).

Dissolved organic matter (DOM) or with other name natural organic matter (NOM) is a complex mixture of organic compounds with different structures. Fulvic and humic acids are the dominant DOM fractions in natural waters. Due to the undefined composition, the rate constants are generally given in $mgC^{-1}\ dm^3\ s^{-1}$ units. Of course, the rate constant strongly depends on the source: in the literature, there are many values for DOM of different origins (e.g., Yuan *et al.* 2022). Here we mention only the value of Guo *et al.* (2017), $4.5 \times 10^4\ mgC^{-1}\ dm^3\ s^{-1}$, which is often used in modeling studies.

CONCLUDING REMARKS

Rate constants of $ClO^{\bullet}$ reactions were collected from the literature and were discussed together with the methods of determination and the reaction mechanisms. Only a small fraction of these rate constants was determined by the absolute method, pulse radiolysis combined with kinetic spectroscopy. The major part was determined by competitive techniques. In another group of experiments, the rate constants were derived in rather complex reaction systems using simulations/modeling or fitting procedures and often involving radical scavenging experiments in the determinations. Quantum chemical calculations were also frequently used to determine $ClO^{\bullet}$ rate constants. The latter methods often gave unrealistic rate constant values. Much fewer rate constants are available in the literature on the reaction of $ClO^{\bullet}$ with organic molecules as on the reactions of other main radical intermediates of the UV/chlorine process, $Cl^{\bullet}$, $^{\bullet}OH$ and $Cl_2^{\bullet-}$.

For most compounds, we found only one published rate constant value. Therefore, we had little possibility to compare the values obtained in different laboratories, eventually employing different techniques. In cases when several rate constant

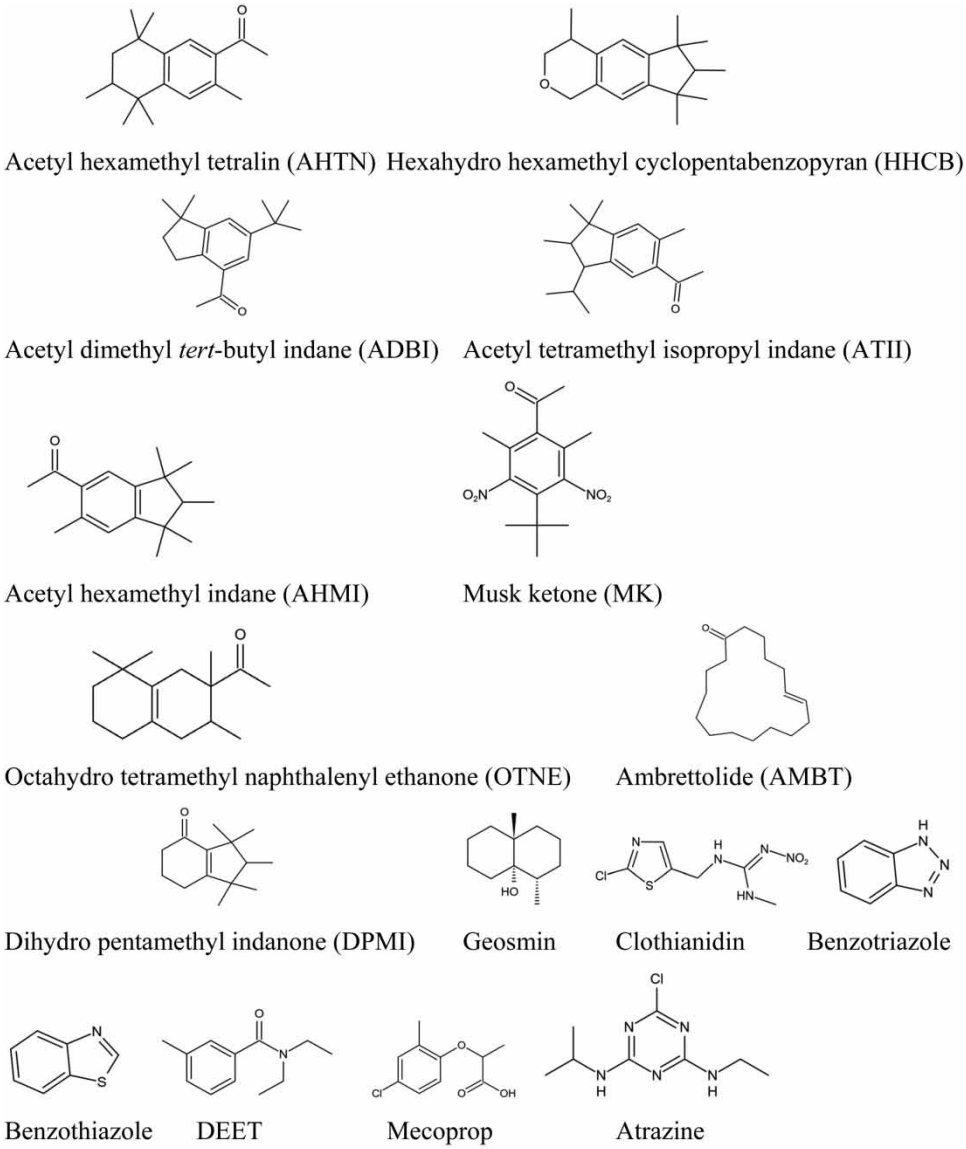

Figure 6 | Miscellaneous compounds.

values were published, we often observed large differences between the values obtained from different sources. The calculated values span a very large range from 10^2 to 10^{10} mol^{-1} dm^3 s^{-1}. The experimentally obtained ones are between 10^5 and 10^{10} mol^{-1} dm^3 s^{-1}. With very few exceptions, the experimental values are well below 1×10^{10} mol^{-1} dm^3 s^{-1}. The latter value is considered to be the diffusion-controlled limit for $ClO^{\bullet}$ (Kovács *et al.* 2022). Therefore, the reaction rate constants are determined by the chemical reactivity, and diffusion limitation has little role. We know very little about the nature of chemical reactions. This is due to the small number of pulsed radiolysis investigations. The transient identification may give direct indications about the reaction mechanism. However, it seems that a basic mechanism is a radical addition to the double bonds (aromatic rings) of organic molecules. In some cases, evidence was given also for SET reaction. There are no direct indications for the participation of H-atom abstraction. The structure dependence of the rate constant values clearly shows an electrophile character similar to the other three radicals playing a major role in the UV/chlorine process. In reactions of phenols, benzoic acids, and anilines, the reactivity strongly increases with deprotonation, i.e. with the increase of electron density on the rings.

Since $ClO^{\bullet}$ reactions play a very important role in the emerging UV/chlorine technology, some standardization of the rate constant measuring techniques and more $k_{ClO^{\bullet}}$ measurements are needed.

ACKNOWLEDGEMENT

This work was supported by the National Office for Research and Development through the Hungarian-Chinese Industrial Research and Development Cooperation Project (No. 2017-2.3.6.-TÉT-CN-2018-00003).

DATA AVAILABILITY STATEMENT

All relevant data are included in the paper or its Supplementary Information.

CONFLICT OF INTEREST

The authors declare there is no conflict.

REFERENCES

Alfassi, Z. B. & Schuler, R. H. 1985 Reaction of azide radicals with aromatic compounds. Azide as a selective oxidant. *Journal of Physical Chemistry* **89**, 3359–3363. https://doi.org/10.1021/j100261a040.

Alfassi, Z. B., Huie, R. E., Mosseri, S. & Neta, P. 1988 Kinetics of one-electron oxidation by the ClO radical. *Radiation Physics and Chemistry* **32**, 85–88. https://doi.org/10.1021/j100298a031.

An, Z., Li, M., Huo, Y., Jiang, J., Zhou, Y., Jin, Z., Xie, J., Zhan, J. & He, M. 2022 The pH-dependent contributions of radical species during the removal of aromatic acids and bases in light/chlorine systems. *Chemical Engineering Journal* **433**, 133493. https://doi.org/10.1016/j.cej.2021.133493.

Armstrong, D. E., Huie, R. E., Koppenol, W. H., Lymar, S. V., Merényi, G., Neta, P., Ruscic, B., Stanbury, D. M., Steenken, S. & Wardman, P. 2015 Standard electrode potentials involving radicals in aqueous solution: inorganic radicals (IUPAC technical report). *Pure and Applied Chemistry* **87**, 1139–1150. https://doi.org/10.1515/pac-2014-0502.

Babic, B., Horvat, A. J. M., Pavlovic, D. M. & Kastelan-Macan, M. 2007 Determination of pK_a values of active pharmaceutical ingredients. *Trends in Analytical Chemistry* **26**, 1043–1061. https://doi.org/10.1016/j.trac.2007.09.004.

Buxton, G. V., Bydder, M. & Salmon, G. A. 1988 Reactivity of chlorine atoms in aqueous solution part 1. The equilibrium $Cl^{\bullet} + Cl^{-} \leftrightarrow Cl_2^{\bullet-}$. *Journal of the Chemical Society, Faraday Transactions* **94**, 653–657. https://doi.org/10.1039/A707377A.

Cai, W.-W., Peng, T., Yang, B., Xu, C., Liu, S., Zhao, J.-L., Gu, F.-L. & Ying, G.-G. 2020 Kinetics and mechanism of reactive radical mediated fluconazole degradation by the UV/chlorine process: experimental and theoretical studies. *Chemical Engineering Journal* **402**, 126224. https://doi.org/10.1016/j.cej.2020.126224.

Cha, Y., Kim, T.-K., Lee, J., Kim, T., Hong, A.-J. & Zoh, K.-D. 2022 Degradation of iopromide during the UV-LED/chlorine reaction: effect of wavelength, radical contribution, transformation products, and toxicity. *Journal of Hazardous Materials* **437**, 129371. https://doi.org/10.1016/j.jhazmat.2022.129371.

Choo, Z.-S., Hsieh, M.-C., Lin, H. H.-H., Yang, J.-S. & Lin, A. Y.-C. 2022 Reactive chlorine species in the enhanced degradation of UV stabilizers during the sunlight/free chlorine process. *Chemosphere* **309** (Pt 1), 136677. https://doi.org/10.1016/j.chemosphere.2022.136677.

De Laat, J. & Stefan, M., 2018 UV/Chlorine process. In: *Advanced Oxidation Processes for Water Treatment, Fundamentals and Application* (Stefan, M. I. ed.). IWA Publishing, London, UK.

Fang, J., Liu, J., Shang, C. & Fan, C. 2018 Degradation investigation of selected taste and odor compounds by a UV/Chlorine advanced oxidation process. *International Journal of Environmental Research and Public Health* **15** (2), 284. https://doi.org/10.3390/ijerph15020284.

Giang, L. T., Phuong, D. T., Thuy, Q. C. & Yen, D. H. 2017 The contribution of free radicals in paracetamol degradation by UV/NaClO. *Vietnam Journal of Chemistry, International Edition* **55**, 720–723. https://doi.org/10.15625/2525-2321.2017-00532.

Guo, K., Wu, Z., Shang, C., Yao, B., Hou, S., Yang, X., Song, W. & Fang, J. 2017 Radical chemistry and structural relationships of PPCP degradation by UV/chlorine treatment. *Environmental Science and Technology* **51**, 10431–10439. https://doi.org/10.1021/acs.est.7b02059.

Guo, K., Wu, Z., Yan, S., Yao, B., Song, W., Hua, Z., Zhang, X., Kong, X., Li, X. & Fang, J. 2018 Comparison of the UV/chlorine and UV/H_2O_2 processes in the degradation of PPCPs in simulated drinking water and wastewater: kinetics, radical mechanism and energy requirements. *Water Research* **147**, 184–194. https://doi.org/10.1016/j.watres.2018.08.048.

Hu, C., Xiong, C., Lin, Y.-L., Zhu, Y., Wang, Q., Xu, L. & Huang, D. 2022 Degradation of 2-phenylbenzimidazole 5-sulfonic acid by UV/chlorine advanced oxidation technology: kinetic model, degradation byproducts and reaction pathways. *Journal of Hazardous Materials* **431**, 128574. https://doi.org/10.1016/j.jhazmat.2022.128574.

Huang, K. & Zhang, H. 2022 A comprehensive kinetic model for phenol oxidation in seven advanced oxidation processes and considering the effects of halides and carbonate. *Water Research* **14**, 100129. https://doi.org/10.1016/j.wroa.2021.100129.

Huie, R. E., Clifton, C. L. & Neta, P. 1991 Electron transfer reaction rates and equilibria of the carbonate and sulfate radical anions. *Radiation Physics and Chemistry* **38**, 477–481. https://doi.org/10.1016/1359-0197(91)90065-A.

Kim, T.-K., Kim, T., Cha, Y. & Zoh, K.-D. 2020 Energy-efficient erythromycin degradation using UV-LED (275 nm)/chlorine process: radical contribution, transformation products, and toxicity evaluation. *Water Research* **185**, 116159. https://doi.org/10.1016/j.watres.2020.116159.

Klaening, U. K., Sehested, K. & Wolff, T. 1984 Ozone formation in laser flash photolysis of oxoacids and oxoanions of chlorine and bromine. *Journal of the Chemical Society, Faraday Transactions* **1** (80), 2969–2979. https://doi.org/10.1039/F19848002969.

Kong, X., Jiang, J., Ma, J., Yang, Y. & Pang, S. 2018a Comparative investigation of X-ray contrast medium degradation by UV/chlorine and UV/H_2O_2. *Chemosphere* **193**, 655–663. https://doi.org/10.1016/j.chemosphere.2017.11.064.

Kong, X., Wu, Z., Ren, Z., Guo, K., Hou, S., Hua, Z., Li, X. & Fang, J. 2018b Degradation of lipid regulators by the UV/chlorine process: radical mechanisms, chlorine oxide radical (ClO•)-mediated transformation pathways and toxicity changes. *Water Research* **137**, 242–250. https://doi.org/10.1016/j.watres.2018.03.004.

Kong, Q., Lei, X., Zhang, X., Cheng, S., Xu, C., Yang, B. & Yang, X. 2020a The role of chlorine oxide radical (ClO˙) in the degradation of polychoro-1,3-butadienes in UV/chlorine treatment: kinetics and mechanisms. *Water Research* **183**, 116056. https://doi.org/10.1016/j.watres.2020.116056.

Kong, X., Wang, L., Wu, Z., Zeng, F., Sun, H., Guo, K., Hua, Z. & Fang, J. 2020b Solar irradiation combined with chlorine can detoxify herbicides. *Water Research* **177**, 115784. https://doi.org/10.1016/j.watres.2020.115784.

Kovács, K., Tóth, T. & Wojnárovits, L. 2022 Evaluation of advanced oxidation processes for ß-blockers degradation: a review. *Water Science and Technology* **85**, 685–705. https://doi.org/10.2166/wst.2021.631.

Lee, Y.-J., Lee, C.-G., Park, J.-J., Moon, J.-K. & Alvarez, P. J. J. 2021 pH-dependent contribution of chlorine monoxide radicals and byproducts formation during UV/chlorine treatment on clothianidin. *Chemical Engineering Journal* **428**, 132444. https://doi.org/10.1016/j.cej.2021.132444.

Lee, W., Shin, J., Lee, M., Choi, Y., Son, H. & Lee, Y. 2022 Elimination efficiency of synthetic musks during the treatment of drinking water with ozonation and UV-based advanced oxidation processes. *Science of the Total Environment* **844**, 156915. https://doi.org/10.1016/j.scitotenv.2022.156915.

Li, M., Mei, Q., Wei, B., An, Z., Sun, J., Xie, J. & He, M. 2021a Mechanism and kinetics of ClO•-mediated degradation of aromatic compounds in aqueous solution: dFT and QSAR studies. *Chemical Engineering Journal* **412**, 128728. https://doi.org/10.1016/j.cej.2021.128728.

Li, M., Mei, Q., Han, D., Wei, B., An, Z., Cao, H., Xie, J. & He, M. 2021b The roles of HO•, ClO• and BrO• radicals in caffeine degradation: a theoretical study. *Science of the Total Environment* **768**, 144733. https://doi.org/10.1016/j.scitotenv.2020.144733.

Li, M., An, Z., Huo, Y., Jiang, J., Zhou, Y., Cao, H. & He, M. 2022 Simulation degradation of bromophenolic compounds in chlorine-based advanced oxidation processes: mechanism, microscopic and apparent kinetics, and toxicity assessment. *Chemosphere* **291**, 133034. https://doi.org/10.1016/j.chemosphere.2021.133034.

Liu, H., Hou, Z., Li, Y., Lei, Y., Xu, Z., Gu, J. & Tian, S. 2021 Modeling degradation kinetics of gemfibrozil and naproxen in the UV/chlorine system: roles of reactive species and effects of water matrix. *Water Research* **202**, 117445. https://doi.org/10.1016/j.watres.2021.117445.

Luo, C., Li, M., Cheng, X., Wu, D., Tan, F., Li, Z., Chen, Y., Yu, F. & Ma, Q. 2022 Degradation of iopamidol by UV365/NaClO: roles of reactive species, degradation mechanism, and toxicology. *Water Research* **222**, 118840. https://doi.org/10.1016/j.watres.2022.118840.

Mertens, R. & von Sonntag, C. V. 1995 Photolysis ((=354nm) of tetrachloroethylene in aqueous solution. *Journal of Photochemistry and Photobiology A: Chemistry* **85**, 1–9. https://doi.org/10.1016/1010-6030(94)03903-8.

Neta, P., Huie, R. E. & Ross, A. B. 1988 Rate constants of the reactions of inorganic radicals in aqueous solution. *Journal of Physics and Chemistry Reference Data* **17**, 1027–1079. https://doi.org/10.1063/1.555808.

Pan, M., Wu, Z., Tang, C., Guo, K., Cao, Y. & Fang, J. 2018 Emerging investigators series: comparative study of naproxen degradation by the UV/chlorine and the UV/H_2O_2 advanced oxidation processes. *Environmental Science: Water Research and Technology* **4**, 1219–1230. https://doi.org/10.1039/C8EW00105G.

Peng, T., Xu, C., Yang, L., Yang, B., Cai, W.-W., Gu, F. & Ying, G.-G. 2022 Kinetics and mechanism of degradation of reactive radical-mediated probe compounds by the UV/Chlorine process: theoretical calculation and experimental verification. *ACS Omega* **7** (6), 5053–5063. https://doi.org/10.1021/acsomega.1c06001.

Perrin, D. D. 1965 *Dissociation Constants of Organic Bases in Aqueous Solution.* Butterworth, London, UK.

Quiroga, S. L. & Perissinotti, L. J. 2005 Reduced mechanism for the 366 nm chlorine dioxide photodecomposition in N_2-saturated aqueous solutions. *Journal of Photochemistry and Photobiology A Chemistry* **171**, 59–67. https://doi.org/10.1016/j.jphotochem.2004.09.006.

Shalaeva, M., Kenseth, J., Lombardo, F. & Bastin, A. 2008 Measurement of dissociation constants (pKa values) of organic compounds by multiplexed capillary electrophoresis using aqueous and cosolvent buffers. *Journal of Pharmacological Sciences* **97**, 2581–2606. https://doi.org/10.1002/jps.21287.

Shi, X. T., Liu, Y. Z., Tang, Y. Q., Feng, L. & Zhang, L. Q. 2018 Kinetics and pathways of bezafibrate degradation in UV/chlorine process. *Environmental Science and Pollution Research International* **25**, 672–682. https://doi.org/10.1007/s11356-017-0461-9.

Shruti Salil, T. 2018 *UV/Chlorine Advanced Oxidation Processes: Factors Influencing P-Cresol Transformation Kinetics*. *Electronic Thesis*, University of Arizona, Tucson, AZ, USA. http://hdl.handle.net/10150/628152 Accessed 12 October 2022.

Sun, P., Lee, W.-N., Zhang, R. & Huang, C.-H. 2016 Degradation of DEET and caffeine under UV/chlorine and simulated sunlight/chlorine conditions. *Environmental Science and Technology* **50**, 13265–13273. https://doi.org/10.1021/acs.est.6b02287.

Sun, Q., Yang, J., Fan, Y., Cai, K., Lu, Z., He, Z., Xu, Z., Lai, X., Zheng, Y., Liu, F., Wang, F. & Sun, Z. 2022 The role of trace N-Oxyl compounds as redox mediator in enhancing antiviral ribavirin elimination in UV/Chlorine process. *Applied Catalysis B: Environmental* **317**, 121709. https://doi.org/10.1016/j.apcatb.2022.121709.

Teo, Y. S., Jafari, I., Liang, F., Jung, Y., Van der Hoek, J. P., Ong, S. & Hu, J. 2022 Investigation of the efficacy of the UV/Chlorine process for the removal of trimethoprim: effects of operational parameters and artificial neural networks modelling. *Science of the Total Environment* **812**, 152551. https://doi.org/10.1016/j.scitotenv.2021.152551.

Wang, L. & Liu, X. 2019 Degradation of aqueous polycyclic musk tonalide by ultraviolet-activated free chlorine. *Processes* **7** (2), 95. https://doi.org/10.3390/pr7020095.

Wang, Y., Couet, M., Gutierrez, L., Allard, S. & Croué, J.-P. 2020 Impact of DOM source and character on the degradation of primidone by UV/chlorine: reaction kinetics and disinfection by-product formation. *Water Research* **172**, 115463. https://doi.org/10.1016/j.watres.2019.115463.

Wang, B., Zhang, Q., Fu, Y., Ran, Z., Crittenden, J. C., Zhang, W. & Wang, H. 2021a Degradation of trimethoprim using the UV/Free chlorine process: influencing factors and optimal operating conditions. *Water* **13**, 1656. https://doi.org/10.3390/w13121656.

Wang, P., Bu, L., Wu, Y., Deng, J. & Zhou, S. 2021b Mechanistic insight into paracetamol transformation in UV/NH_2Cl process: experimental and theoretical study. *Water Research* **194**, 116938. https://doi.org/10.1016/j.watres.2021.116938.

Wang, J., Deng, J., Du, E. & Guo, H. 2022a Re-evaluation of radical-induced differentiation in UV-based advanced oxidation processes (UV/hydrogen peroxide, UV/peroxydisulfate, and UV/chlorine) for metronidazole removal: kinetics, mechanism, toxicity variation, and DFT studies. *Separation and Purification Technology* **301**, 121905. https://doi.org/10.1016/j.seppur.2022.121905.

Wang, Z., Li, J., Song, W., Ma, R., Yang, J., Zhang, X., Huang, F. & Dong, W. 2022b Rapid degradation of atrazine by a novel advanced oxidation process of bisulfite/chlorine dioxide: efficiency, mechanism, pathway. *Chemical Engineering Journal* **445**, 136558. https://doi.org/10.1016/j.cej.2022.136558.

Wojnárovits, L. & Takács, E. 2021 Rate constants of dichloride radical anion reactions with molecules of environmental interest in aqueous solution, a review. *Environmental Science and Pollution Research* **28**, 41552–44157. https://doi.org/10.1007/s11356-021-14453-w.

Wojnárovits, L. & Takács, E. 2022 Rate constants of chlorine atom reactions with organic molecules in aqueous solutions, an overview. *Environmental Science and Pollution Research* **29**, 55492–55513. https://doi.org/10.1007/s11356-022-20807-9.

Wu, Z., Guo, K., Fang, J., Yang, X., Xiao, H., Hou, S., Kong, X., Shang, C., Yang, X., Meng, F. & Chen, L. 2017 Factors affecting the roles of reactive species in the degradation of micropollutants by the UV/chlorine process. *Water Research* **126**, 351–360. https://doi.org/10.1016/j.watres.2017.09.028.

Yang, T., Mai, J., Wu, S., Liu, C., Tang, L., Mo, Z., Zhang, M., Guo, L., Liu, M. & Ma, J. 2021 UV/chlorine process for degradation of benzothiazole and benzotriazole in water: efficiency, mechanism and toxicity evaluation. *Science of the Total Environment* **760**, 144304. https://doi.org/10.1016/j.scitotenv.2020.144304.

Ye, B., Liu, Z., Zhu, X., Wu, H., Liang, Z., Wang, W., Wu, Q., Hu, H. & Zhang, X. 2021 Degradation of atrazine (ATZ) by ammonia/chlorine synergistic oxidation process. *Chemical Engineering Journal* **415**, 128841. https://doi.org/10.1016/j.cej.2021.128841.

Yin, K., Li, T., Zhang, T., Zhang, Y., Yang, C. & Luo, S. 2022 Degradation of organic filter 2-Phenylbenzidazole-5-Sulfonic acid by light-driven free chlorine process: reactive species and mechanisms. *Chemical Engineering Journal* **430**, 132684. https://doi.org/10.1016/j.cej.2021.132684.

Yuan, D., Liu, G., Qi, F., Wang, J., Kou, Y., Cui, Y., Bai, M. & Li, X. 2022 Kinetic study on degradation of micro-organics by different UV-based advanced oxidation processes in EfOM matrix. *Environmental Science and Pollution Research* **29**, 45314–45327. https://doi.org/10.1007/s11356-022-19087-0.

Zhang, Z., Chuang, Y.-H., Szczuka, A., Ishida, K. P., Roback, S., Plumlee, M. H. & Mitch, W. A. 2019 Pilot-scale evaluation of oxidant speciation, 1,4-dioxane degradation and disinfection byproduct formation during UV/hydrogen peroxide, UV/free chlorine and UV/chloramines advanced oxidation process treatment for potable reuse. *Water Research* **164**, 114939. https://doi.org/10.1016/j.watres.2019.114939.

Zhang, H., Li, Z., Zhou, X., Lu, X., Gu, H. & Ma, J. 2022 Insight into the performance of UV/chlorine/TiO2 on carbamazepine degradation: the crucial role of chlorine oxide radical ($ClO^{\bullet}$). *Science of the Total Environment* **853**, 158345. https://doi.org/10.1016/j.scitotenv.2022.158345.

Zheng, W., Zhu, L., Liang, S., Ye, J., Yang, X., Lei, Z., Yan, Z., Li, Y., Wei, C. & Feng, C. 2020 Discovering the importance of $ClO^{\bullet}$ in a coupled electrochemical system for the simultaneous removal of carbon and nitrogen from secondary coking wastewater effluent. *Environmental Science and Technology* **54**, 9015–9024. https://doi.org/10.1021/acs.est.9b07704.

Zheng, Y., Xie, H., Sun, B., Zhang, J. & Wang, W. 2022 The altered effects of chloride on the treatment efficiency of $SO_4^{\bullet-}$-based AOPs by other background water constituents. *Chemical Engineering Journal* **441**, 135914. https://doi.org/10.1016/j.cej.2022.135914.

Zhou, S., Zhang, W., Sun, J., Zhu, S., Li, K., Meng, X., Luo, J., Shi, Z., Zhou, D. & Crittenden, J. C. 2019 Oxidation mechanisms of the UV/free chlorine process: kinetic modelling and quantitative activity relationships. *Environmental Science and Technology* **53**, 4335–4345. https://doi.org/10.1021/acs.est.8b06896.

Zhu, S., Tian, Z., Wang, P., Zhang, W., Bu, L., Wu, Y., Dong, B. & Zhou, S. 2021 The role of carbonate radicals on the kinetics, radical chemistry, and energy requirement of UV/chlorine and UV/H_2O_2 processes. *Chemosphere* **278**, 130499. https://doi.org/10.1016/j.chemosphere.2021.130499.

First received 30 November 2022; accepted in revised form 31 March 2023. Available online 12 April 2023